

Charge carrier dynamics and relaxation in (polyethylene oxide–lithium-salt)-based polymer electrolyte containing 1-butyl-1-methylpyrrolidinium bis(trifluoromethylsulfonyl)imide as ionic liquid

A. Karmakar and A. Ghosh*

Department of Solid State Physics, Indian Association for the Cultivation of Science, Jadavpur, Kolkata 700032, India

(Received 31 August 2011; published 2 November 2011)

In this paper we report the dynamics of charge carriers and relaxation in polymer electrolytes based on polyethylene oxide (PEO), lithium bis(trifluoromethylsulfonyl)imide (LiTFSI) and 1-butyl-1-methylpyrrolidinium bis(trifluoromethylsulfonyl)imide (BMPTFSI) ionic liquid prepared by solution cast technique. It has been observed that the incorporation of BMPTFSI into PEO-LiTFSI electrolyte is an effective way for increasing the amorphous phase to a large extent. It has also been observed that both the glass transition and melting temperatures decrease with the increase of BMPTFSI concentration. The ionic conductivity of these polymer electrolytes increases with the increase of BMPTFSI concentration. The highest ionic conductivity obtained at 25 °C is $\sim 3 \times 10^{-4}$ S cm⁻¹ for the electrolyte containing 60 wt % BMPTFSI and ethylene oxide (EO)/Li ratio of 20. The temperature dependence of the dc conductivity and the hopping frequency show Vogel-Tamman-Fulcher type behavior indicating a strong coupling between the ionic and the polymer chain segmental motions. The frequency dependence of the ac conductivity exhibits a power law with an exponent n which decreases with the increase of temperature. The scaling of the ac conductivity indicates that relaxation dynamics of charge carriers follows a common mechanism for all temperatures and BMPTFSI concentrations. We have also presented the electric modulus data which have been analyzed in the framework of a Havriliak-Negami equation and the shape parameters obtained by the analysis show slight temperature dependence, but change sharply with BMPTFSI concentration. The stretched exponent β obtained from Kohlrausch-Williams-Watts fit to the modulus data is much lower than unity signifying that the relaxation is highly nonexponential. The decay function obtained from analysis of experimental modulus data is highly asymmetric with time.

DOI: [10.1103/PhysRevE.84.051802](https://doi.org/10.1103/PhysRevE.84.051802)

PACS number(s): 36.20.-r, 61.25.H-, 82.45.Gj, 66.10.Ed

I. INTRODUCTION

There is a growing interest in the studies of solid polymer electrolytes (SPEs) for their applications in electrochemical devices such as rechargeable solid-state lithium ion batteries, fuel cells, capacitors, and several new applications including biocompatible devices [1–4]. Among various SPEs polyethylene oxide (PEO)-lithium salt (LiX) complexes [5] are more attractive as they can offer number of advantages in terms of their high energy density, better cycle ability, and safety to be used as electrolytes in solid-state batteries [1]. But the application of these SPEs is limited due to their low ionic conductivity at room temperature because the highly symmetrical repeating ethylene oxide units tend to crystallize. For practical application the conductivity of these SPEs should be $>10^{-4}$ S cm⁻¹, which is achieved only at temperatures higher than 60 °C (above the melting point of PEO), i.e., when PEO is in an amorphous state. It is believed that for obtaining sufficiently high ionic conductivity, large amorphous regions of these complexes are necessary, as Li⁺ ions conduct only in the amorphous regions.

To increase the ionic conductivity different approaches have been adopted. A number of reports [6,7] have demonstrated that the addition of plasticizers such as tetraethylene glycol, ethylene carbonate, propylene carbonate, etc., into the polymer matrix increases their conductivity considerably by preventing crystallization of the polymer-salt phase and promoting the

host polymer chain to a more flexible condition. However, they suffer from several drawbacks, such as decomposition, volatilization, reaction towards lithium metal electrode, and also the deterioration of the mechanical properties. Another approach involves the addition of ceramic nanoparticles such as Al₂O₃, TiO₂ [8] and inclusion of inorganic nanoparticles [9,10] as fillers to form composite electrolytes to improve the conductivity considerably. Although a substantial improvement of the conductivity has been observed in these composite electrolytes, the enhancement is still far below what would be necessary to consider them suitable for practical applications at room temperature.

In the last few years ionic liquids (ILs) have gained a considerable attention from the researchers for their use as electrolytes or electrolyte components for better performance. ILs, consisting only of organic cation and inorganic anion, possess many favorable conditions such as good thermal and electrochemical stability, high ionic conductivity, a wide electrochemical voltage window, negligible vapor pressure, and nonflammability [11,12]. Depending on the cations, imidazolium- [13], pyrrolidinium- [14,15], piperidinium- [16,17], etc., based ILs have been extensively investigated as electrolyte components for battery and capacitor applications and the performance has been enhanced considerably. In polymer electrolytes these ionic liquids not only act as the supplier of additional charge carriers but also play the role of plasticizers as well [18].

In this work we have embedded 1-butyl-1-methylpyrrolidinium bis(trifluoromethylsulfonyl)imide (BMPTFSI) as ionic liquid in PEO- lithium bis(trifluoromethylsulfonyl)imide

*sspaga@iacs.res.in

(LiTFSI) electrolyte. To gain an understanding of the conduction mechanism, ion-ion interaction, etc., we have studied electrical conductivity and relaxation in these BMPTFSI ionic liquid-based PEO-LiTFSI electrolytes.

II. EXPERIMENTAL DETAILS

The chemicals PEO, LiTFSI, and BMPTFSI (Sigma-Aldrich) were dried in vacuum prior to use. Both the lithium salt and the ionic liquid have a common anion to make it chemically compatible. For the preparation of free-standing polymer electrolyte films a standard solution cast technique has been used. For the preparation of PEO-LiTFSI electrolyte, appropriate amounts of PEO (MW = 400 000) and LiTFSI were dissolved in acetonitrile under stirring condition. The molar ratio of the ethylene oxide segments to the lithium ions was maintained at ethylene oxide (EO)/Li = 20. Then appropriate amounts of BMPTFSI were mixed with the above mentioned slurry under stirring condition. The concentration of BMPTFSI was varied from 10 wt % to 60 wt %. After stirring for 24 h at room temperature, the solutions became very thick due to solvent evaporation. Finally, they were cast in polytetrafluoroethylene (PTFE) containers and the solvent was allowed to evaporate slowly in ambient condition to form homogeneous free-standing films. The films were further dried in vacuum for ~36 h at 55 °C to remove any residual solvent. Beyond the concentration of 60 wt % BMPTFSI the obtained films show a sticky nature and the mechanical properties become very poor.

X-ray diffraction (XRD) patterns of the as-prepared films were recorded in an x-ray diffractometer (D8 Advance, Bruker AXS) using Cu- K_{α} radiation (0.154-nm wavelength) at a scan rate of 1° min. Thermal properties of the films were investigated by differential scanning calorimetry (DSC) at a heating scan rate of 10 °C/min in TA instrument (Model Q2000) in N₂ atmosphere. Electrical measurements such as capacitance and conductance were carried out at various temperatures in an anhydrous environment in the frequency range 10 Hz–2 MHz using a RLC meter (QuadTech, model 7600). A conductivity cell containing two stainless steel blocking electrodes was used for the ac impedance measurements. The measurements at different temperatures were done by placing the sample cell in a cryostat with a temperature stability of 0.10 K.

III. RESULTS AND DISCUSSION

Figure 1(a) shows the x-ray diffraction patterns of PEO-LiTFSI and PEO-LiTFSI-BMPTFSI electrolytes. Two strong diffraction peaks (at $2\theta = 19^{\circ}$ and 23.5°) are observed for PEO-LiTFSI electrolyte. These peaks are the characteristic peaks of PEO due to its crystalline phase. The intensity of these diffraction peaks decreases when BMPTFSI is added to the PEO-LiTFSI electrolyte. The peak intensity further decreases with the increase of BMPTFSI concentration and is the lowest for the highest BMPTFSI concentration (60 wt %). These results can be interpreted in terms of the criteria of Hodge *et al.* [19], where a correlation between the height of the peak and the degree of crystallinity has been established. The decrease of the intensity is a clear indication that the amorphous phase of PEO increases with

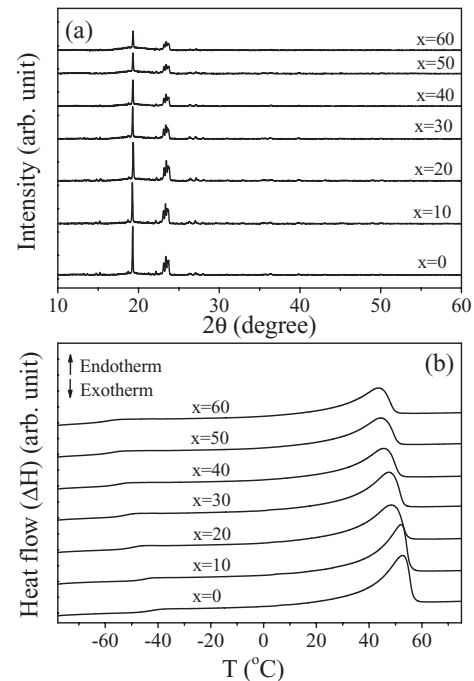


FIG. 1. (a) X-ray diffraction patterns for different compositions of PEO-LiTFSI- x wt % BMPTFSI electrolytes. (b) DSC thermograms for different compositions of PEO-LiTFSI- x wt % BMPTFSI electrolytes.

the addition of BMPTFSI and the amorphous phase further increases with the increase of BMPTFSI concentration. These results indicate that the addition of BMPTFSI in PEO-LiTFSI electrolyte has locally changed the ordered form of PEO to a disordered form. In other words, the volume fraction of amorphous phase of PEO polymer electrolyte increased with the increasing amount of BMPTFSI into the polymer matrix. Figure 1(b) illustrates the DSC measurements performed on PEO-LiTFSI and PEO-LiTFSI-BMPTFSI electrolytes. The large, sharp endothermic peak observed is assigned to the melting of PEO phases and the heat capacity change at lower temperature is attributed to the glass transition temperature (T_g) of the PEO. The thermodynamic parameters such as glass transition temperature, melting temperature (T_m), and melting enthalpy (ΔH_m) have been obtained from the DSC traces and are summarized in Table I. From the table it is observed that T_g gradually decreases with the increase of BMPTFSI concentration. The decrease of T_g suggests that the addition of BMPTFSI increases the flexibility of the polymer chain. Also with the increase of BMPTFSI concentration the melting temperature decreases and the broadness of the melting peak increases which infers an increased amount of amorphous phase of PEO. The percentage of crystalline phase of PEO (X_c) has been calculated from the following relation:

$$X_c = \Delta H_m / \Delta H_{PEO}, \quad (1)$$

where ΔH_m is the melting enthalpy of the sample and ΔH_{PEO} is the melting enthalpy (namely 213.7 J/g) of completely crystalline PEO [20]. The calculated value of X_c is presented in Table I. It is observed in the table that the amorphous phase increases with the increase of BMPTFSI concentration. Zhu *et al.* also observed similar results by incorporating

TABLE I. Thermal parameters of PEO-LiTFSI- BMPTFSI electrolytes obtained from DSC.

BMPTFSI concentration	T_g (°C) (±2)	T_m (°C) (±2)	ΔH (J/g)	% X_c
0	-42.23	52.71	67.69	31.68
10	-45.28	52.11	63.32	29.63
20	-49.77	48.51	58.90	27.56
30	-52.26	47.53	56.45	26.42
40	-55.13	45.66	50.35	23.56
50	-57.48	44.52	47.24	22.11
60	-59.32	43.69	44.59	20.87

imidazolium-based ionic liquid in the PEO-LiTFSI electrolyte [21]. Thus it is expected that the interaction of the ions, present in the ionic liquid, with the ether oxygen of PEO and Li^+ ions prevents the crystallization of PEO and produces an increased amount of amorphous phase [22], supporting the results obtained from XRD.

The most important parameter for the polymer electrolytes is its ionic conductivity. Typical complex impedance plots for PEO-LiTFSI electrolyte containing 10 wt % BMPTFSI at different temperatures are shown in Fig. 2(a). Inclined spikes obtained at low frequencies are due to the electrode-electrolyte polarization. Similar plots have been observed for other

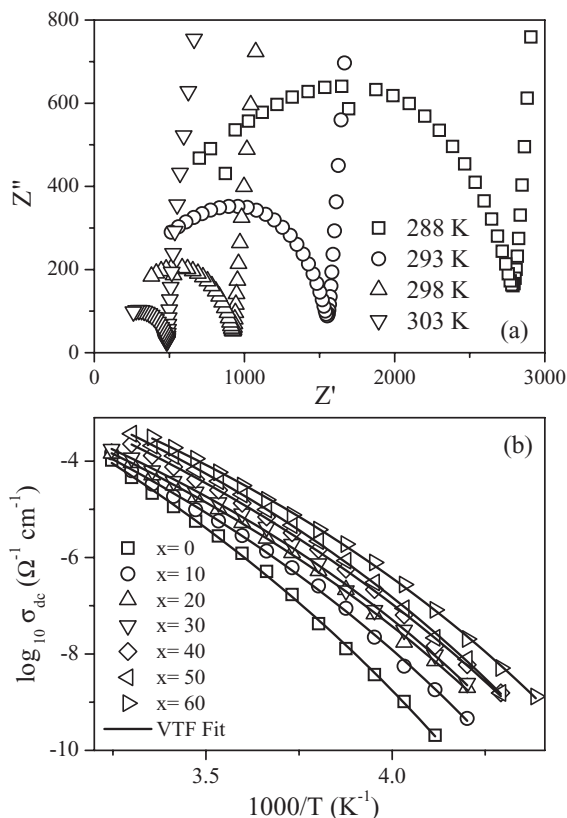


FIG. 2. (a) Complex impedance plots at different temperatures for PEO-LiTFSI-20 wt % BMPTFSI polymer electrolytes. (b) Variation of dc conductivity with reciprocal temperature for different compositions of PEO-LiTFSI- x wt % BMPTFSI electrolytes. The solid lines are VTF fits [Eq. (2)] to the experimental data.

samples. The dc electrical conductivity, obtained from these complex impedance plots, is shown in Fig. 2(b) as a function of reciprocal temperature for different PEO-LiTFSI-BMPTFSI electrolytes. It is noted that the dc conductivity follows Vogel-Tamman-Fulcher (VTF) [23–25] behavior. The VTF equation, which has been effectively used to describe various dynamical processes in glassy and polymeric systems [26,27], is expressed as

$$f(T) = AT^{-1/2} \exp \left[\frac{-E_a}{K_B(T - T_0)} \right], \quad (2)$$

where A is the preexponential factor, K_B is the Boltzman constant, E_a is the pseudoactivation barrier related to the critical free volume for ion transport, T_0 is the Vogel scaling temperature where the configurational entropy or the critical volume becomes zero, and T is the absolute temperature. Generally, the value of $(T_g - T_0)$ is of the order of 50 K for salt-polymer complexes [26] and ionic liquids [12]. The conductivity data of all the electrolytes studied here have been fitted to Eq. (2) using nonlinear least squares fits. The solid lines in Fig. 2(b) show such VTF fits. The parameters E_a and T_0 obtained from fits are shown in Table II. A reasonably good fit of the conductivity to the VTF relation over a wide range of temperatures clearly indicates that the ionic conductivity is favored as a result of the segmental motion of the polymer chain in the matrix resulting from the free volume change with temperature [26,28], and there exists a strong relation between the conductivity and the polymer chain segmental motions [26,28].

The variation of dc conductivity with BMPTFSI concentration at different temperatures is shown in Fig. 3. It is observed that the dc conductivity progressively increases with the increase of BMPTFSI concentration for all temperatures. Also it is observed in Fig. 2(b) that the addition of BMPTFSI to PEO-LiTFSI electrolytes enhances the dc conductivity without changing its temperature-dependence profile. This suggests that though the carrier concentration is influenced by the addition of BMPTFSI in this polymeric electrolyte system, the intrinsic mechanism for the ionic conduction remains unchanged [29]. The dc conductivity of PEO-LiTFSI obtained at 25 °C increases by an order for 60 wt % BMPTFSI. The addition of BMPTFSI not only introduces extra ions for conduction in the matrix but the anions provided by BMPTFSI assist Li^+ ions to be freed partially or fully by interacting with the coordination between Li^+ ions and O atoms of PEO segments; thus a larger number of charge carriers is produced with improved charge migration [30]. Thus, incorporation of BMPTFSI is an effective way of enhancing the ionic conductivity of PEO-based electrolytes.

The ac conductivity spectra at different temperatures for a composition are shown in Fig. 4. In the figure three distinct regions are clearly observed. At low frequency the conductivity drops down due to the accumulation of charge at the electrode-electrolyte interfaces. In the intermediate region the conductivity is independent of frequency and is equal to the dc conductivity arising from the random diffusion of the ionic charge carriers via activated hopping. At higher frequencies the probability for the ions to go to another favorable site and to fall back to their original site increases [26,31]. This high probability is responsible for the higher conductivity at

TABLE II. VTF fitting parameters obtained for PEO-LiTFSI- BMPTFSI electrolytes.

BMPTFSI Concentration	From dc conductivity data		From crossover frequency data	
	E_a (eV) (± 0.002)	T_0 (K) (± 5)	E_a (eV) (± 0.002)	T_0 (K) (± 5)
0	0.054	144.2	0.052	140.4
10	0.041	149.1	0.041	152.9
20	0.039	147.4	0.042	151.9
30	0.033	155.1	0.039	153.1
40	0.039	144.3	0.041	146.1
50	0.037	149.8	0.037	149.1
60	0.035	147.4	0.036	147.5

higher frequencies, showing dispersion. It is observed that the crossover from the frequency-independent dc region to the frequency-dependent dispersive region shifts to higher frequencies with increase in temperature. A similar nature of the conductivity spectra has been observed for the samples containing different BMPTFSI concentrations.

The power law formalism has been very successful in explaining the ac conductivity spectra in disordered materials including ion conducting glasses, ion conducting polymer electrolytes, etc. [32–36]. In the power law formalism [32–34] the ac conductivity, $\sigma'(\omega)$ is expressed by

$$\sigma'(\omega) = \sigma_{dc} [1 + (\omega/\omega_c)^n], \quad (3)$$

where σ_{dc} is the dc conductivity, ω_c is the crossover frequency which is closely related to the hopping frequency, and n is the power law exponent which measures the interaction between the mobile charge carriers. The above model has been successfully employed to analyze the ac conductivity spectra for obtaining clear knowledge about the ion dynamics in some polymer electrolytes [31,37]. The conductivity data at different temperatures have been fitted to Eq. (3) using a nonlinear least squares technique using σ_{dc} , ω_c , and n as

variable parameters. The best fits are shown by solid lines in Fig. 4. A good agreement between the power law model and the experimental data at various temperatures is observed in this figure. We have observed that the values of σ_{dc} obtained from the fits (shown in Fig. 3) match perfectly with those obtained from complex impedance plots. The variation of the crossover frequency, obtained from the fit, with reciprocal temperature is shown in Fig. 5. It is observed that the crossover frequency follows a VTF relation [Eq. (2)]. The solid lines in Fig. 5 show the best fits and the parameters obtained from the fits are summarized in Table II. It is noted that the parameters are very close to those obtained from the dc conductivity. This indicates that the charge transfer mechanism based on ion migration coupled with the segmental motion of the polymer host contributes to the ionic conductivity in these polymer electrolytes [29].

Temperature dependence of the parameter n provides information about the interaction between the mobile charge carriers. In general, the value of n is less than unity. However, the values of n greater than unity have been observed for some polymeric materials [38]. There are some reports on ceramic and glassy systems [39,40] where the value of n decreases with

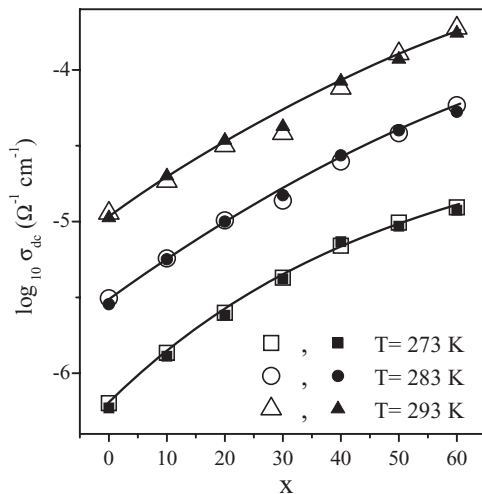


FIG. 3. Variation of dc conductivity obtained from the complex impedance plot (open symbol) and dc conductivity obtained from the fits of Eq. (3) to the conductivity spectra (solid symbol) at different temperatures with BMPTFSI concentration for PEO-LiTFSI-BMPTFSI electrolytes. Solid lines are guides to the eye.

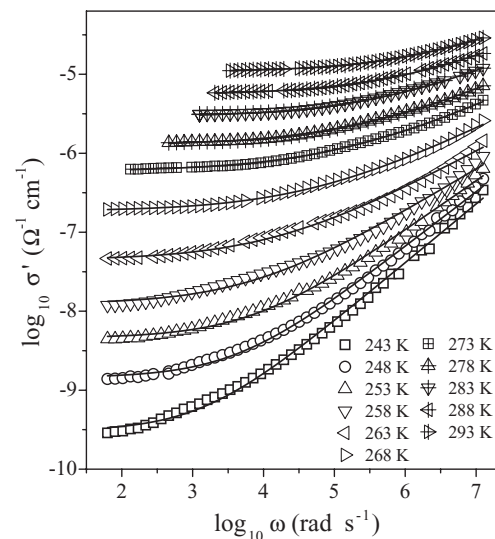


FIG. 4. Ac conductivity spectra at different temperatures for PEO-LiTFSI-10 wt % BMPTFSI electrolytes. Solid lines are the fits of Eq. (3) to the experimental data.

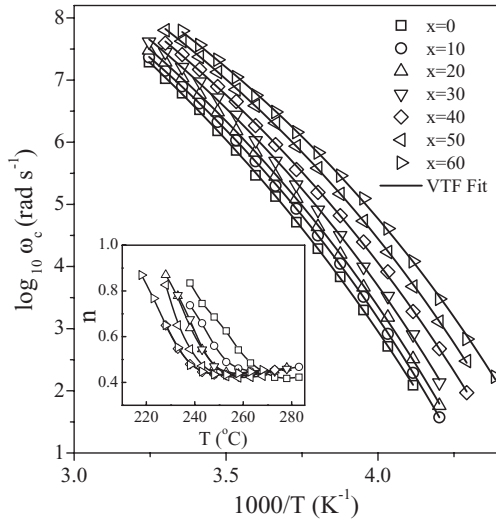


FIG. 5. Dependence of crossover frequency on reciprocal temperature for different compositions of PEO-LiTFSI- x wt % BMPTFSI electrolytes. The solid lines are VTF fits [Eq. (2)] to the experimental data. Inset of the figure shows the dependence of frequency exponent (n) with temperature and solid lines are a guide to the eye.

the increase of temperature due to the interaction between the mobile ions available in the matrix. The values of n , obtained from the above fits, might be affected by the “window effect” [41,42]. For obtaining a meaningful exponent only those data sets have been considered for which $\omega_{\max}/\omega_c > 10$ and in that case the “window effect” is negligible. In our case $\omega_{\max} = 2\pi f_{\max}$, where $f_{\max} = 2$ MHz and we have taken only those values of n for which $\omega_{\max}/\omega_c > 10$. The variation of n with temperature is shown in the inset of Fig. 5 for all samples. It is noted that at low temperatures the parameter n has a high value, but the value of n decreases with the increase of temperature and attains nearly a constant value.

To gain insight into the temperature and composition dependence of the ion dynamics the scaling behavior of the conductivity spectra has been studied. The procedure of scaling of the conductivity spectra has been outlined elsewhere [43]. The results at different temperatures for PEO-LiTFSI-10 wt % BMPTFSI electrolytes are shown in Fig. 6(a). It is observed that all the spectra at different temperatures merge to a common master curve. The near-perfect overlap of the spectra indicates that the polymer electrolytes obey the time-temperature superposition principle. The scaling results for different BMPTFSI concentrations of PEO-LiTFSI electrolytes at a particular temperature are shown in Fig. 6(b). In Fig. 6(b), we note that all the conductivity spectra of different BMPTFSI concentration are nearly scaled to a common master curve. Similar results were also obtained for other temperatures. Thus the nature of relaxation dynamics of charge carriers in the PEO-LiTFSI-BMPTFSI electrolytes follows a common mechanism throughout the entire temperature and BMPTFSI concentration ranges.

The electric modulus has been used to analyze and interpret electrical relaxation data in a wide variety of materials [44–46]. This formalism provides significant insights on charge transport processes such as mechanism

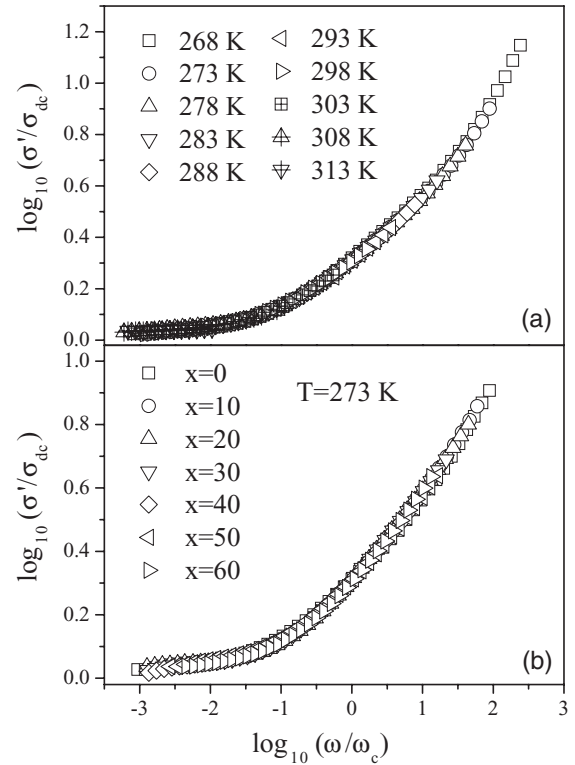


FIG. 6. (a) Scaling of the conductivity spectra for different temperatures for PEO-LiTFSI-10 wt % BMPTFSI electrolytes. (b) Scaling of the conductivity spectra at $T = 273$ K for PEO-LiTFSI-BMPTFSI electrolytes with different BMPTFSI concentration.

of conductivity relaxation as a function of frequency and temperature. In the modulus formalism [46], an electric modulus M^* is defined as the inverse of the complex dielectric permittivity ϵ^* :

$$M^* = 1/\epsilon^* = M' + jM'', \quad (4)$$

where M' and M'' are the real and imaginary parts of the complex modulus M^* . Figure 7 shows the frequency dependence of M' and M'' spectra at different temperatures for PEO-LiTFSI-60 wt % BMPTFSI electrolyte. It is observed that M' gradually increases with the increase of frequency. In fact, M' should saturate at M_∞ at higher frequencies, which is not observed due to limitation in our experiment. In the M'' spectra, distinct peaks are observed. The region to the left side of the peak is where the ions are mobile over long distances and the region to the right is where the ions are spatially confined to their potential wells. The frequency where the peak occurs is indicative of a change from short-range to long-range mobility at decreasing frequency. As the temperature is increased the movement of the charge carriers becomes faster, leading to decreased relaxation time, with a consequent shift of the peak value of M'' towards higher frequencies. This behavior suggests that the relaxation is thermally activated, and charge carrier hopping is taking place. The conductivity relaxation frequency ω_m , corresponding to M''_{\max} , gives the most probable conductivity relaxation time τ_m and was obtained from the condition $\omega_m \tau_m = 1$ [46]. We also observe that M'' spectra are much broader than that of the ideal Debye case (1.14

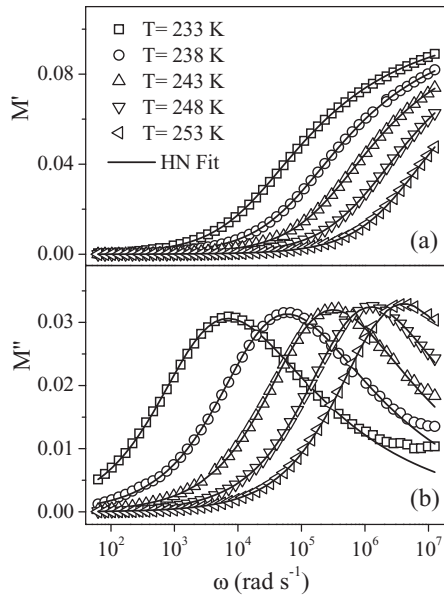


FIG. 7. Frequency dependence of the (a) real part (M') and (b) imaginary part (M'') of complex electric modulus M^* for PEO-LiTFSI-60 wt % BMPTFSI electrolytes. The solid lines are HN fits [Eq. (5)] to the experimental data.

decades) and show asymmetric and skewed nature towards the high-frequency sides of the maxima. Such a broad nature of the peaks can be interpreted as a consequence of distribution of relaxation times and clearly indicates the occurrence of non-Debye relaxation in the present samples. The same nature of temperature dependence M'' has been observed for other BMPTFSI concentrations.

To obtain information about non-Debye relaxation the isotherms for M'' in the frequency domain have been conveniently analyzed in the framework of the empirical Havriliak-Negami (HN) function [47,48] given by

$$M^* = M_\infty + (M_s - M_\infty) \left[\frac{1}{1 + (i\omega\tau_{\text{HN}})^\alpha} \right]^\gamma, \quad (5)$$

where M_s and M_∞ are, respectively, the low- and high-frequency limiting values of the electric modulus, τ_{HN} is the relaxation time, and α and γ are the shape parameters which describe the symmetric and asymmetric broadening of the complex modulus function, respectively, taking values $0 < \alpha, \gamma \leq 1$. The Debye equation is recovered when both α and γ are unity.

The present experimental data have been fitted to the HN function [Eq. (5)] and the best fits are shown as solid lines in Fig. 7. The parameters obtained from the fits are shown in Table III. Figure 8(a) shows the reciprocal temperature dependence of the relaxation time τ_{HN} for different samples. It is clearly observed that the relaxation time follows VTF-type behavior. It is also noted that the relaxation time decreases with increasing temperature and also with increasing BMPTFSI concentration. Figure 8(b) shows the temperature variation of the shape parameters α and γ obtained from the fits. It is noted that both α and γ are almost independent of temperature varying slightly at lower temperatures indicating a slight initial increase in asymmetry of the peaks with

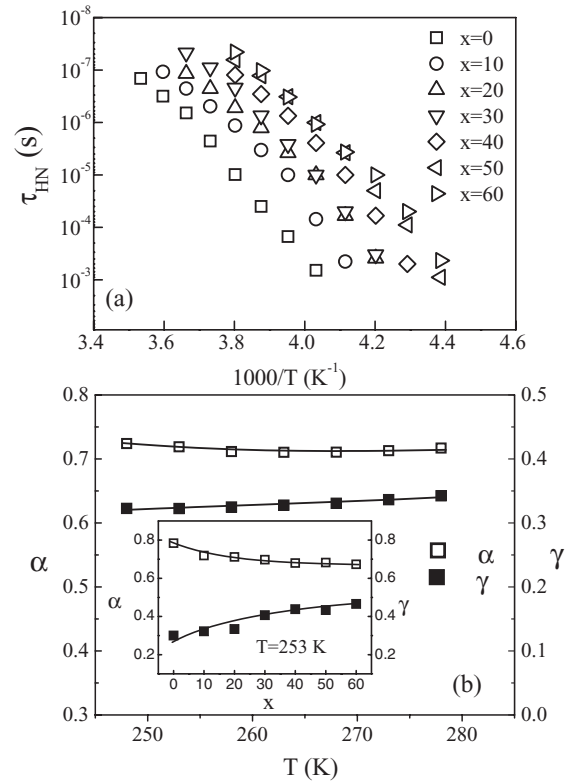


FIG. 8. (a) Reciprocal temperature dependence of relaxation time τ_{HN} for different compositions of PEO-LiTFSI- x wt % BMPTFSI electrolytes. (b) Variation of HN shape parameter α and γ with temperature and inset of the figure shows the same but with BMPTFSI concentration at $T = 253$ K. The solid lines are a guide to the eye.

the increase of temperature. Similar behavior has also been observed for other samples. The inset of Fig. 8(b) shows the variation of α and γ with BMPTFSI concentration. It is observed that the shape parameter α decreases with the increase of BMPTFSI concentration. However, the shape parameter γ shows the opposite nature. These observations indicate that the asymmetry of the modulus peaks increases with the increase of BMPTFSI concentration. The increase of asymmetry may arise from the inclusion of extra ions provided by the BMPTFSI ionic liquid [49].

The complex modulus M^* can also be expressed in terms of Fourier transform of a decay function $\varphi(t)$ given by [46]

$$M^* = M_\infty \left[1 - \int_0^\infty \exp(-i\omega t) \left(\frac{d\varphi}{dt} \right) dt \right], \quad (6)$$

where the function $\varphi(t)$ describes the decay of the electric field within ionic conductors in the time domain. In the case of non-Debye behavior, $\varphi(t)$ can be well approximated by the Kohlrausch-Williams-Watts (KWW) decay function given by [50,51]

$$\varphi(t) \approx \exp \left[- \left(\frac{t}{\tau_{\text{KWW}}} \right)^\beta \right], \quad (7)$$

where τ_{KWW} is the characteristic relaxation time and β is the stretched exponent ($0 < \beta \leq 1$), which indicates the deviation from ideal Debye relaxation. A quantitative analysis of the

TABLE III. Relaxation time τ_{HN} , HN asymmetric parameter α and γ , KWW relaxation time τ_{KWW} , and stretched exponent β for PEO-LiTFSI- BMPTFSI electrolytes.

BMPTFSI concentration	$\log_{10} \tau_{\text{HN}}$ (s) (± 0.05) (258 K)	α (± 0.02)(258 K)	γ (± 0.02)(258 K)	$\log_{10} \tau_{\text{KWW}}$ (s) (± 0.05)(258 K)	β (± 0.02)
0	-4.39	0.78	0.30	-5.39	0.30
10	-5.47	0.71	0.32	-6.42	0.30
20	-5.89	0.71	0.34	-6.78	0.31
30	-6.13	0.69	0.41	-6.81	0.33
40	-6.54	0.69	0.43	-7.16	0.35
50	-6.89	0.68	0.44	-7.51	0.35
60	-6.99	0.67	0.46	-7.55	0.36

modulus data in the time domain can be obtained by calculating the function $\varphi(t)$ using the inverse transform of Eq. (6) such as

$$\varphi(t) = \frac{2}{\pi} \int_0^{\infty} \frac{M''}{\omega M_{\infty}} \cos(\omega t) d\omega. \quad (8)$$

Here it is sufficient to use M'' in the calculation of $\varphi(t)$, since real and imaginary parts of M^* are connected by the Kramers-Krönig transform. The experimental decay curves $\varphi(t)$ obtained from such analysis are plotted in Fig. 9(a) for different compositions. The decay function is found to be asymmetric with respect to time. The KWW function [Eq. (7)] has been used to fit the experimental $\varphi(t)$ curves

and the solid lines in Fig. 9(a) show such fits. The values of τ_{KWW} and stretched exponent β , obtained from such fits, have been shown in Table III for different samples. The variation of β with temperature is shown in Fig. 9(b) and the inset of this figure shows the variation of β with BMPTFSI concentration. From these figures we observe that the values of β do not vary significantly with temperature, but increase slightly with BMPTFSI concentration. The values of β are also much lower than unity signifying that the relaxation is highly nonexponential. The low values of β also suggest a cooperative motion of the ions in the electrolyte, i.e., the jump of a mobile ion cannot be treated as an isolated event. The jump of the ion from one equilibrium site to another causes a time-dependent movement of other ions in the surroundings [52].

The relationship between the HN and KWW parameters can be expressed as the following approximation [49,53]:

$$\log_{10}(\tau_{\text{HN}}/\tau_{\text{KWW}}) \approx 2.6(1 - \beta)^{0.5} \exp(-3\beta), \quad (9a)$$

$$\beta \approx (\alpha\gamma)^{1/1.23}. \quad (9b)$$

For the present samples it is noted that these relations hold well, further suggesting that either of the representations of the HN function or the KWW function is valid and has the same physical significance.

IV. CONCLUSIONS

The amorphous phase of PEO-LiTFSI-BMPTFSI electrolytes increases with BMPTFSI concentration due to the hindrance of the crystallization tendency of PEO chains caused by the interaction of BMPTFSI with PEO. Both the glass transition and melting temperatures decrease with the increase of BMPTFSI concentration. The dc conductivity as well as the hopping frequency show VTF-type behavior and increase with the increase of BMPTFSI concentration. The highest ionic conductivity obtained at 25 °C was found to be $3 \times 10^{-4} \text{ S cm}^{-1}$ for the electrolyte containing 60 wt % of ionic liquid and EO/Li ratio of 20. The frequency exponent n decreases with the increase in temperature. Using the scaling of ac conductivity data we have observed that the addition of BMPTFSI to PEO-LiTFSI electrolyte does not change the nature of the relaxation dynamics of charge carriers in these electrolytes and is independent of temperature and BMPTFSI concentration. The shape parameters α and γ obtained from the

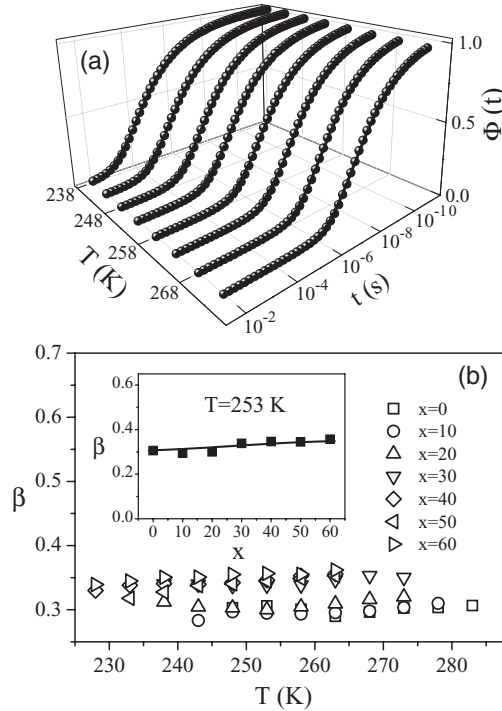


FIG. 9. (a) Temperature and time dependence of the KWW decay function $\varphi(t)$, PEO-LiTFSI-20 wt % BMPTFSI electrolytes. Solid lines are the best fit to Eq. (7). (b) Variation of β with temperature for different compositions of PEO-LiTFSI- x wt % BMPTFSI electrolytes. Inset of the figure shows the variation of β with BMPTFSI concentration at $T = 253$ K. Solid lines are a guide to the eye.

fitting of the Havriliak-Negami equation to the modulus data show a slight temperature dependency suggesting an increase in asymmetry of the peaks, but a sharp change has been observed as BMPTFSI concentration is increased, indicating an interaction of the extra ions provided by BMPTFSI with the polymer chain. The low value of stretched exponent β obtained from the Kohlrausch-Williams-Watts fit to the modulus data show the highly nonexponential nature of the relaxation

peak. The obtained decay function is highly asymmetric in time.

ACKNOWLEDGMENTS

A.K. acknowledges the Council of Scientific and Industrial Research, Government of India, for providing support (via Grant No. 09/080(0573)/2007-EMR-I) for the work.

-
- [1] J. M. Tarascon and M. Armand, *Nature (London, UK)* **414**, 359 (2001).
- [2] C. A. Furtado, P. P. De Souza, G. Goulart Silva, T. Matencio, and J. M. Pernaut, *Electrochim. Acta* **46**, 1629 (2001).
- [3] K. A. Mowery, M. H. Schoenfisch, N. Baliga, J. A. Wahr, and M. E. Meyerhoff, *Electroanalysis* **11**, 681 (1999).
- [4] Z. Gadjourova, Y. G. Andreev, D. P. Tunstall, and P. G. Bruce, *Nature (London, UK)* **412**, 520 (2001).
- [5] Z. Stoeva, I. Martin-Litas, E. Staunton, Y. G. Andreev, and P. G. Bruce, *J. Am. Chem. Soc.* **125**, 4619 (2003).
- [6] R. Frech and S. Chintapalli, *Solid State Ionics* **85**, 61 (1996).
- [7] Y. T. Kim and E. S. Smotkin, *Solid State Ionics* **149**, 29 (2002).
- [8] F. Croce, G. B. Appetecchi, L. Persi, and B. Scrosati, *Nature (London, UK)* **394**, 456 (1998).
- [9] B. Scrosati, F. Croce, and L. Persi, *J. Electrochem. Soc.* **147**, 1718 (2000).
- [10] C.-W. Nan, L. Fan, Y. Lin, and Q. Cai, *Phys. Rev. Lett.* **91**, 266104 (2003).
- [11] B. Singh and S. S. Sekhon, *Chem. Phys. Lett.* **414**, 34 (2005).
- [12] M. Galiński, A. Lewandowski, and I. Stepniak, *Electrochim. Acta* **51**, 5567 (2006).
- [13] J. Reiter, J. Vondrák, J. Michálek, and Z. Mička, *Electrochim. Acta* **52**, 1398 (2006).
- [14] G. B. Appetecchi, G. T. Kim, M. Montanino, M. Carewska, R. Marcilla, D. Mecerreyes, and I. De Meazza, *J. Power Sources* **195**, 3668 (2010).
- [15] J. H. Shin, W. A. Henderson, and S. Passerini, *J. Electrochem. Soc.* **152**, A978 (2005).
- [16] S. Fang, Z. Zhang, Y. Jin, L. Yang, S. I. Hirano, K. Tachibana, and S. Katayama, *J. Power Sources* **196**, 5637 (2011).
- [17] A. Triolo, O. Russina, B. Fazio, G. B. Appetecchi, M. Carewska, and S. Passerini, *J. Chem. Phys.* **130**, 164521 (2009).
- [18] H. Ohno, M. Yoshizawa, and W. Ogihara, *Electrochim. Acta* **48**, 2079 (2003).
- [19] R. M. Hodge, G. H. Edward, and G. P. Simon, *Polymer* **37**, 1371 (1996).
- [20] X. Li and S. L. Hsu, *J. Polym. Sci., Polym. Phys. Ed.* **22**, 1331 (1984).
- [21] C. Zhu, H. Cheng, and Y. Yang, *J. Electrochem. Soc.* **155**, A569 (2008).
- [22] J. H. Shin, W. A. Henderson, C. Tizzani, S. Passerini, S. S. Jeong, and K. W. Kim, *J. Electrochem. Soc.* **153**, A1649 (2006).
- [23] H. Vogel, *Z. Phys.* **22**, 645 (1921).
- [24] G. Tamman and W. Hesse, *Z. Anorg. Allg. Chem.* **156**, 245 (1926).
- [25] G. S. Fulcher, *J. Am. Ceram. Soc.* **8**, 339 (1925).
- [26] B. Natesan, N. K. Karan, and R. S. Katiyar, *Phys. Rev. E* **74**, 042801 (2006).
- [27] R. Ribeiro, G. Goulart Silva, and N. D. S. Mohallem, *Electrochim. Acta* **46**, 1679 (2001).
- [28] B. Wang, S. Q. Li, and S. J. Wang, *Phys. Rev. B* **56**, 11503 (1997).
- [29] W. A. Castro, V. H. Zapata, R. A. Vargas, and B. E. Mellander, *Electrochim. Acta* **53**, 1422 (2007).
- [30] J.-W. Choi, G. Cheruvally, Y.-H. Kim, J.-K. Kim, J. Manuel, P. Raghavan, J.-H. Ahn, K.-W. Kim, H.-J. Ahn, D. S. Choi, and C. E. Song, *Solid State Ionics* **178**, 1235 (2007).
- [31] P. Basak, S. V. Manorama, R. K. Singh, and O. Parkash, *J. Phys. Chem. B* **109**, 1174 (2004).
- [32] D. P. Almond, G. K. Duncan, and A. R. West, *Solid State Ionics* **8**, 159 (1983).
- [33] D. P. Almond and A. R. West, *Solid State Ionics* **9-10**, 277 (1983).
- [34] D. P. Almond and A. R. West, *Nature (London, UK)* **306**, 456 (1983).
- [35] A. K. Jonscher, *Nature (London, UK)* **267**, 673 (1977).
- [36] M. Cutroni, A. Mandanici, P. Mustarelli, C. Tomasi, and M. Federico, *J. Non-Cryst. Solids* **307-310**, 963 (2002).
- [37] A. Karmakar and A. Ghosh, *J. Appl. Phys.* **110**, 034101 (2011).
- [38] A. N. Papanthassiou, I. Sakellis, and J. Grammatikakis, *Appl. Phys. Lett.* **91**, 122911 (2007).
- [39] A. Ghosh, *Phys. Rev. B* **41**, 1479 (1990); **42**, 5665 (1990).
- [40] J. C. Dyre and T. B. Schroöder, *Rev. Mod. Phys.* **72**, 873 (2000).
- [41] H. Jain and C. H. Hsieh, *J. Non-Cryst. Solids* **172-174**, 1408 (1994).
- [42] D. L. Sidebottom, *J. Non-Cryst. Solids* **244**, 223 (1999).
- [43] A. Ghosh and A. Pan, *Phys. Rev. Lett.* **84**, 2188 (2000); S. Bhattacharya and A. Ghosh, *Phys. Rev. B*, **70** 172203 (2004).
- [44] M. J. Sanchis, M. Carsí, P. Ortiz-Serna, G. Domínguez-Espinosa, R. Díaz-Calleja, E. Riande, L. Alegría, L. Gargallo, and D. Radić, *Macromolecules* **43**, 5723 (2010).
- [45] B. Deb and A. Ghosh, *J. Phys. Chem. C* **115**, 14141 (2011).
- [46] P. B. Macedo, C. T. Moynihan, and R. Bose, *Phys. Chem. Glasses* **13**, 171 (1972).
- [47] G. Molnár, S. Cobo, T. Mahfoud, E. J. M. Vertelman, P. J. V. Koningsbruggen, P. Demont, and A. Bousseksou, *J. Phys. Chem. C* **113**, 2586 (2009).
- [48] S. Havriliak and S. Negami, *Polymer* **8**, 161 (1967).

- [49] F. Kremer and A. Schönhals, *Broadband Dielectric Spectroscopy* (Springer: Berlin, 2003).
- [50] R. Kohlrausch, Ann. Phys. (Leipzig) **12**, 393 (1847).
- [51] G. Williams and D. C. Watts, *Trans. Faraday Soc.* **66**, 80 (1970).
- [52] J. M. Réau, S. Rossignol, B. Tanguy, J. M. Rojo, P. Herrero, R. M. Rojas, and J. Sanz, *Solid State Ionics* **74**, 65 (1994).
- [53] F. Alvarez, A. Alegria, and J. Colmenero, *Phy. Rev. B* **44**, 7306 (1991).